Fossil brachiopod identification using a new deep convolutional neural network

Haizhou Wang [a,b,*], Chufan Li [c], Zhifei Zhang [d], Stephen Kershaw [e], Lars E. Holmer [d,f], Yang Zhang [a,b], Keyi Wei [a,b], Peng Liu [g]

[a] State Key Laboratory of Petroleum Resources and Prospecting, China University of Petroleum (Beijing), Beijing 102249, China
[b] College of Geosciences, China University of Petroleum (Beijing), 102249, China
[c] School of Science, Beijing University of Posts and Telecommunications, Beijing 100876, China
[d] State Key Laboratory of Continental Dynamics, Shaanxi Key Laboratory of Early Life and Environments, Department of Geology, Northwest University, Xi'an 710069, China
[e] Insitute for the Environment and Health Sciences, Brunel University, Uxbridge, Middlesex UB8 3PH, UK
[f] Department of Earth Sciences, Palaeobiology, Uppsala University, Villavägen 16, SE-75236 Uppsala, Sweden
[g] College of Safety Science and Engineering, Xi'an University of Science and Technology, Xi'an, Shaanxi 710054, China

ARTICLE INFO

ABSTRACT

The identification of brachiopods requires specialist knowledge held by a limited number of researchers and is very time-consuming. The new technique of deep learning by artificial intelligence offers promising tools to break these shackles to develop computer automatic identification. However, we found that the traditional convolution neural network is not sufficient to automatically identify brachiopod species. Thus, we propose a new tailored Transpose Convolutional Neural Network (TCNN) in order to automatically identify brachiopod fossils with high efficiency. In this network, we add an "upsampling" Transpose Convolutional Layer and synthesize the data of this layer with the data of a Convolutional Layer to fully mix the small and large scales features extracted by the neural network. Compared with the traditional Convolution Neural Network (CNN), the Transpose Convolutional Neural Network (TCNN) can achieve a high identification accuracy using a smaller training data set of images of brachiopods. Results from this study show that the TCNN can achieve 98%, 98% and 97% identification accuracy respectively, with training data sets of 400 images of 3 species, 484 images of 4 species and 630 images of 5 species. In contrast, the traditional CNN can achieve only a low identification accuracy (67%) with 400 images of 3 species and requires 3000 images per 3 species to achieve a 95% identification accuracy. For most of brachiopod species, it is almost an impossible task to collected thousands of samples and as more brachiopod species are fitted into automatic identification, it is significant to have a reliable network which can achieve high accuracy on a small data set. In summary, the TCNN is a more efficient neural network that could be better applied to automatically identify brachiopod fossils.

1. Introduction

The identification of fossils by traditional methods comprises careful visual study and measurements in comparison with a standard identified sample (the type species). Depending on the fossil group studied, although identification can be made using hand specimens, in many cases photographs of specimens are sufficient, as long as they are complete and show the full range of features of the fossil studied. Any fossils that have features which can be fully captured on photographs are suitable for image analysis. There are many fossil groups that have identification characters which are demonstrated using photographs, and one of these, the Brachiopoda, make an important tool in stratigraphy and palaeoecology in the Palaeozoic Era of geological time. However, identification of brachiopods requires specialist knowledge held by a limited number of researchers. Thus if it is possible to identify brachiopods using automatic methods, then the results would have considerable value in geological investigations. Photographs of brachiopod shells which are fully visible in sedimentary rocks show all the key identification characters on bedding planes, suitable for automatic methods as long as they can be imaged accurately and with high enough resolution for pixels to contain critical information on intensity (and colour using an RGB classification) that will allow the image to be appropriately analyzed. Thus, high-resolution and high-contrast photographs of brachiopods may allow recognition of the contrast changes in adjacent

pixels across the photograph of the shell, to recognize boundaries of shell components and their shapes; if the results are compared with a standard dataset of images (the type species), the possibility of using machine-learning techniques may aid identification.

There are two major advantages of machine-based identification of fossils: a) increase in speed of identification to provide a valuable aid for a specialist; b) the system may be used by non-specialists to obtain identifications. If the system can be made to operate at a high level of accuracy, then it may become a reliable taxonomic tool that could be applied to a wide range of fossil organisms.

In this study we explore the application of machine-learning techniques to brachiopods, using the sophisticated method called deep learning, that employs neural networks to measure and analyze the image components and makes predictions of identification. This study therefore aims to achieve a workable automatic identification system of brachiopods using neural networks.

2. Methods and materials

Of the various types of neural network (Goodfellow et al., 2014; Hinton and Salakhutdinov, 2006; Hochreiter and Schmidhuber,
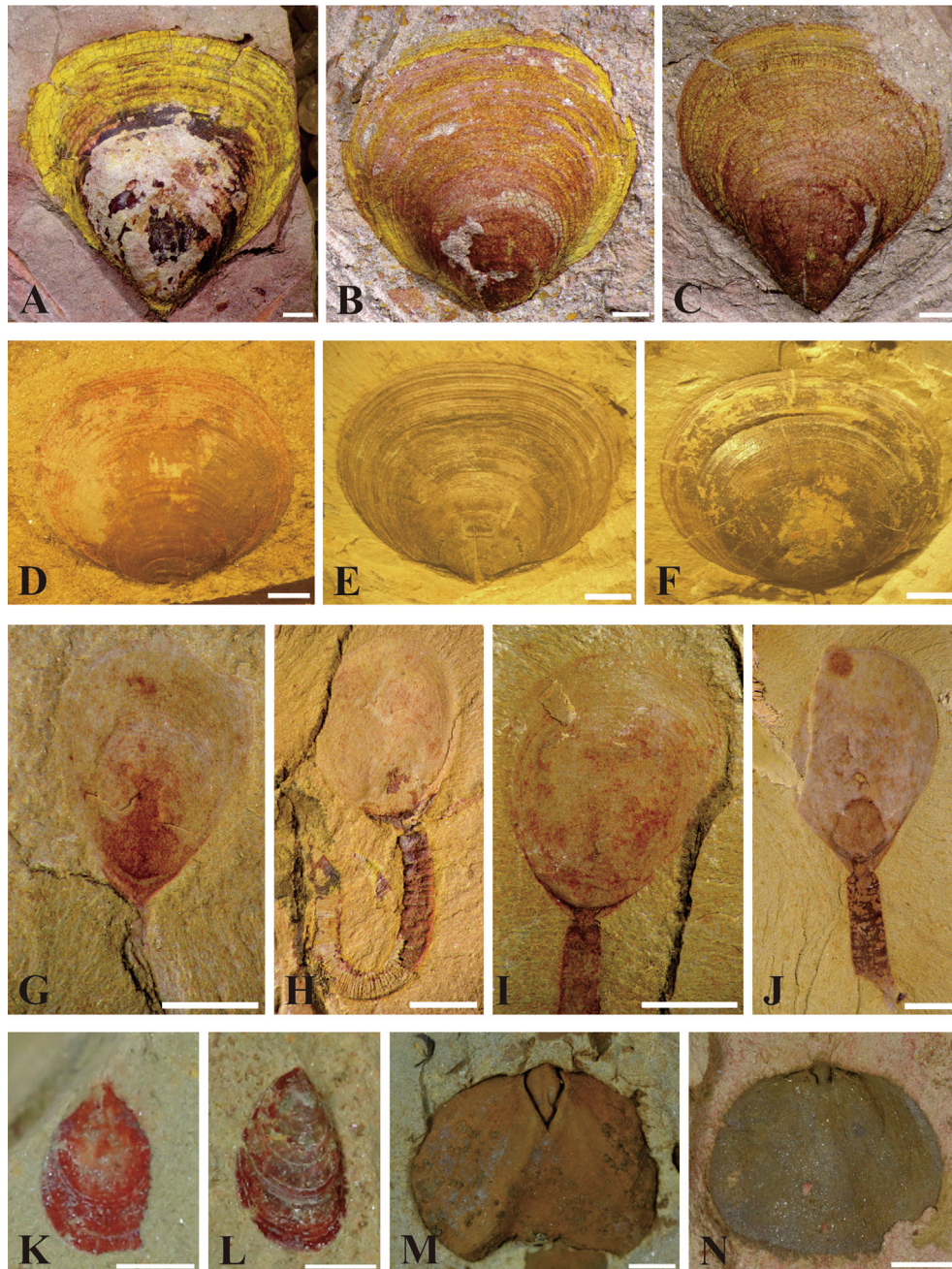

Fig. 1. Brachiopods from the Lower Cambrian Yu'anshan Formation and the Upper Cambrian Guole Formation, China. **A-C**, *Palaeobolus yunnanensis, Scale bars = 2 mm*; **A**, HJS004, ventral external mould; **B**, HJS007-1, dorsal external mould; **C**, HJS077, ventral external mould. **D-F**, *Diandongia pista, Scale bars = 2 mm*; **D**, JS0100A, dorsal external mould; **E**, JS0338A, Ventral external mould; **F**, JS0354A, dorsal external mould. **G-J**, *Eoglossa chengjiangensis*, Scale bars = 2 mm; **G**, JS0112A, a highly compressed specimen showing the imprint of dorsal interior and indistinct ventral pseudointerarea; **H**, JS0131B, a compressed specimen with interior dorsal valve imprint on top. The pedicle, twice as long as shell length, is well preserved and has a third dimension; **I**, JS0288A, exterior view of dorsal valve and interior view of ventral pseudointerarea; **J**, MF0318B, a compressed specimen with interior dorsal valve imprint showing an oval visceral area. **K, L**, *Obolidae get. Et* sp. *indet*. Scale bars = 1 mm; **K**, DB3-O-16, ventral internal mould; **L**, DB3-O-68, ventral internal mould. **M, N**, *Palaeostrophia jingxiensis* Scale bars = 2 mm; **M**, DB3-Pa-123, ventral internal mould; **N**, DB3-Pa-312–1, dorsal internal mould.

1997; Lecun et al., 1998; Salakhutdinov et al., 2007; Silver et al., 2016), the method selected here is the convolutional neural network (CNN), designed to capture data from images and process them to recognize patterns, thus recognize objects. Convolutional in this system is derived from the term convolute and works using a series of layers of information extracted from pixels of images of the subject, that are then built up to produce output that can be compared with identified fossils, leading to identification of the sample material.

Since the CNN was invented (Lecun et al., 1998), it has been widely adopted in deep learning and thus widely used in image classification (i.e., in this case identification of the brachiopod species), target detection (i.e., recognition of the location of the target object) and semantic segmentation (i.e., recognition of the object and its shape). In recent years, a group of classical convolutional neural network models are have been produced, such as VGG16 (Simonyan and Zisserman, 2014), ResNet (He et al., 2016), YOLO (Redmon et al., 2016) and FCN (Long et al., 2015). The application of those models dramatically promoted the development of deep learning and played a significant role in visual recognition tasks. However, those models were constructed based on very large datasets with a huge number of training images, for which fossil specimens are too problematic to analyze (Le et al., 2011). When we applied those models to automatically identify some types of our fossil records, the system lacks sufficient training data for classification (Krizhevsky et al., 2017). Consequently, a large fossil collection presents a significant problem for analysis and taxa recognition by CNN methods, because there need to be sufficient numbers of each taxon in order to achieve satisfactory reliability of identification. In this work we created a new highly efficient automatic fossil-identification model, using the Transpose Convolutional Neural Network (TCNN) mode, valid for a relatively small number of training images.

The TCNN mode was inspired by FCN (Long et al., 2015) and U-NET models (Ronneberger et al., 2015). We add the transpose convolutional layer to our model and mix it with a convolutional layer to fully mix the small and large scale features extracted by the neural network (Jia et al., 2014). This significant transpose convolutional layer is widely used in semantic segmentation, but is rarely used in pure image classification tasks (Long et al., 2015; Ronneberger et al., 2015). After testing the TCNN model based on photos of our brachiopod fossil samples, we found the TCNN mode could significantly reduce the number of the training images, while maintaining a high accuracy of identification.

We run the TCNN mode in the computer with a Nvidia RTX2080Ti GPU which proved to have enough computer capability to run the TCNN program for our dataset. The software environment is Windows 10 installed with a program called "miniconda" which is a programming environment base on Python language. In the "miniconda" Program, we installed the TensorFlow 2.0 framework which is a deep learning framework in which the neural network can be trained by GPU (Abadi, 2016) and installed the "Jupyter" compiler, which is the program used to write the TCNN source code and run the code to carry out deep learning.

In the TCNN source code, we initialized each weight matrix W by GlorotNormal method (Glorot and Bengio, 2010). Each bias vector b is initialized to 0. Each model is trained for 500 training epochs on the Nvidia RTX2080Ti GPU (Cui et al., 2016). The learning rate for the Adam optimizer is 0.001 (Kingma and Ba, 2014). We also use ReduceLROnPlateau callback function, monitor='val_loss', factor = 0.5, patience = 10, min_lr = 0.00001 (Le et al., 2011). After a lot of experiments, we set the learning rate to 0.0003 and the loss function is sparse categorical cross-entropy.

The sample materials for testing the TCNN mode were five different species of Cambrian brachiopods collected from mudstone. All the samples are impression fossils on the mudstone, some of

them with detailed soft-part body preservation. Most of the samples have intact shell shapes, but some of them are fragmented. The samples were all photographed and constitute a package of dataset with 3716 brachiopod photos. The dataset contains 1294 photos of *Eoglossa chengjiangensis* (Zhang et al., 2004; Wang et al., 2014), 1075 photos of *Diandongia pista* (Zhang et al., 2003), 731 photos of *Palaeobolus yunnanensis* (Zhang, 2014), 470 photos of *Palaeostrophia jingxiensis* and 146 photos of *Obolidae gen. et* sp. *indet* (Fig. 1). Among those five species, *Eoglossa chenjiangensis* and *Diandongia pista* are most common species in the Chengjiang biota. *Palaeobolus yunnanensis* is abundant in the Malong biota. *Palaeostrophia jingxiensis* and *Obolidae gen. et* sp. *indet* (Zhan et al., 2010) are common in the Guole biota. However, most of our testing and analyzing for the TCNN mode was based on photos of *Eoglossa chenjiangensis*, *Diandongia pista* and *Palaeobolus yunnanensis*, due to the limited number of available samples of *Palaeostrophia jingxiensis* and *Obolidae gen. et* sp. *indet*. The former three brachiopods are all the members of Lingulata, which means they have the same characteristics at class level and makes them very hard to be classified by non-specialists. The latter two brachiopods photos were used for only helping expand the TCNN mode to the bigger scale of neural network, to see if it has potential to be applied to species identification of more brachiopods. All the samples were mixed together without designating whether they are ventral or dorsal valves, and whether they have a pedicle or not. Thus the TCNN is used to extract as much of the different features as it can, in order to make a judgement of which species is represented.

3. TCNN architecture

The structure of the neural network and the detail explanation of key layers are shown in Figs. 2, 3 and 4. Prior to image capture for the input layer in the TCNN process, we resized all the photos to RGB 256 × 256-pixel images. Our TCNN mode uses eight convolution layers as a subsampling process and the number of convolution kernel is 32, 32, 64, 64, 128, 128, 256, 256 (same as the traditional Neural Network). The Batch Normalization layer is used after each convolutional layer to increase training speed while reducing overfitting (Ioffe and Szegedy, 2015; Li et al., 2019). After each two convolutional layers and two Batch Normalization layers, the maxpooling layer is used to expand the view of the neural network (Giusti et al., 2014). We add one
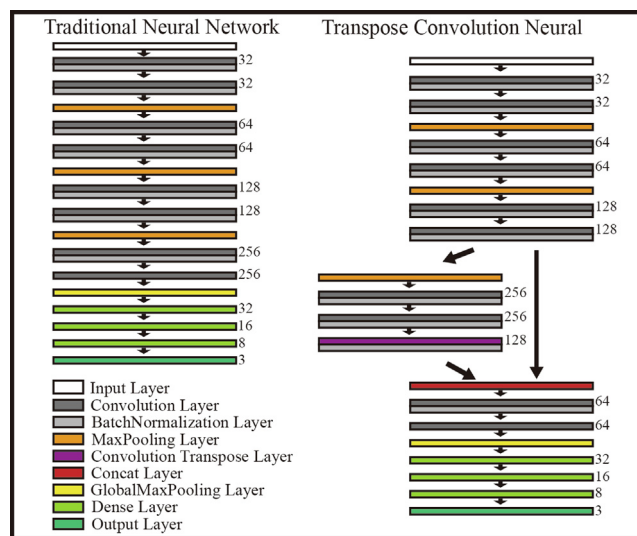

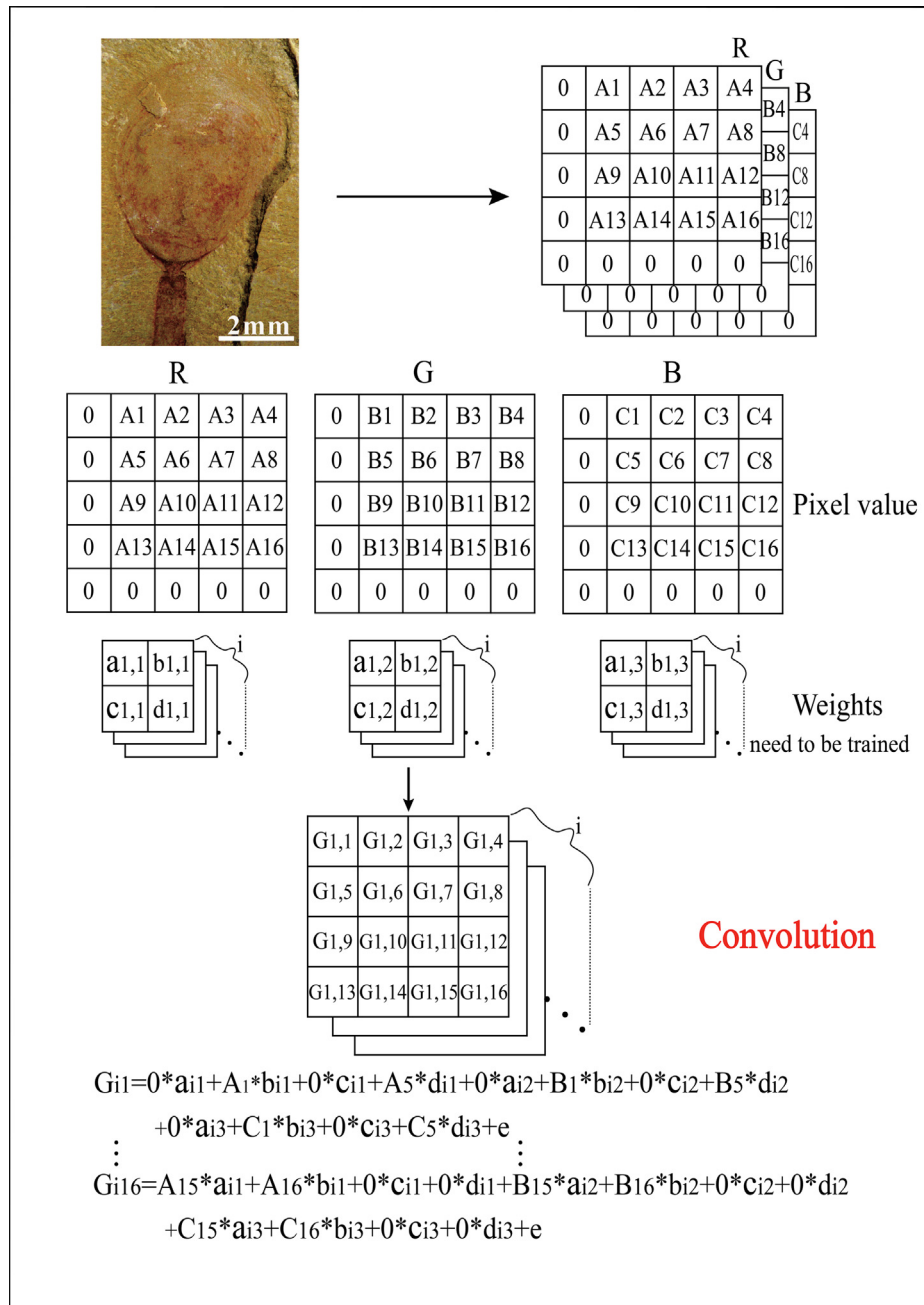**Fig. 2.** The structure of the traditional CNN and the TCNN model.

Fig. 3. Detailed schematic diagram of the Convolution layer.

transpose convolution layer after the eighth Batch Normalization layer which has 128 transpose convolution kernels. The Batch Normalization layer is also added after the transpose convolution layer. We mix the output of the ninth Batch Normalization layer with the output of the sixth Batch Normalization layer by concat method (In the following text, we call the layer executing concat method as concat layer). Then, we add two convolutional layers, a Batch Normalization layer, and a GlobalMaxpooling layer after the concat layer (Shen et al., 2015). Finally, we used four fully connected layers for the final classification. The number of neurons in the fully connected layer was 32, 16, 8, 3. The activation function for the output layer is softmax and the rest layers are ReLU (max $(0, x)$). The convolution kernel size is 3×3 and the transpose convolutional kernel size is 2×2. The stride of the transpose convolution operation is 2.

4. Testing and results

We use 3,100 photos of three types of brachiopods, *Eoglossa chenjiangensis*, *Diandongia pista* and *Palaeobolus yunnanensis* and set up five comparison experiments to test both our TCNN mode and the traditional mode. Before starting the training, 100 photos were randomly and evenly selected as the unique test set. Then we randomly chose 400 photos, 500 photos, 1000 photos, 2000 photos and all 3000 photos as different training data sets. Afterwards, we applied the TCNN mode and the traditional mode to run training on those training data sets. In the end, we use the test set to obtain the identifying accuracy of each compared experiment. As shown in Fig. 5, the accuracy of the TCNN model is always higher than the traditional mode. Moreover, our TCNN model can maintain a high accuracy at 98%, even if the number of training
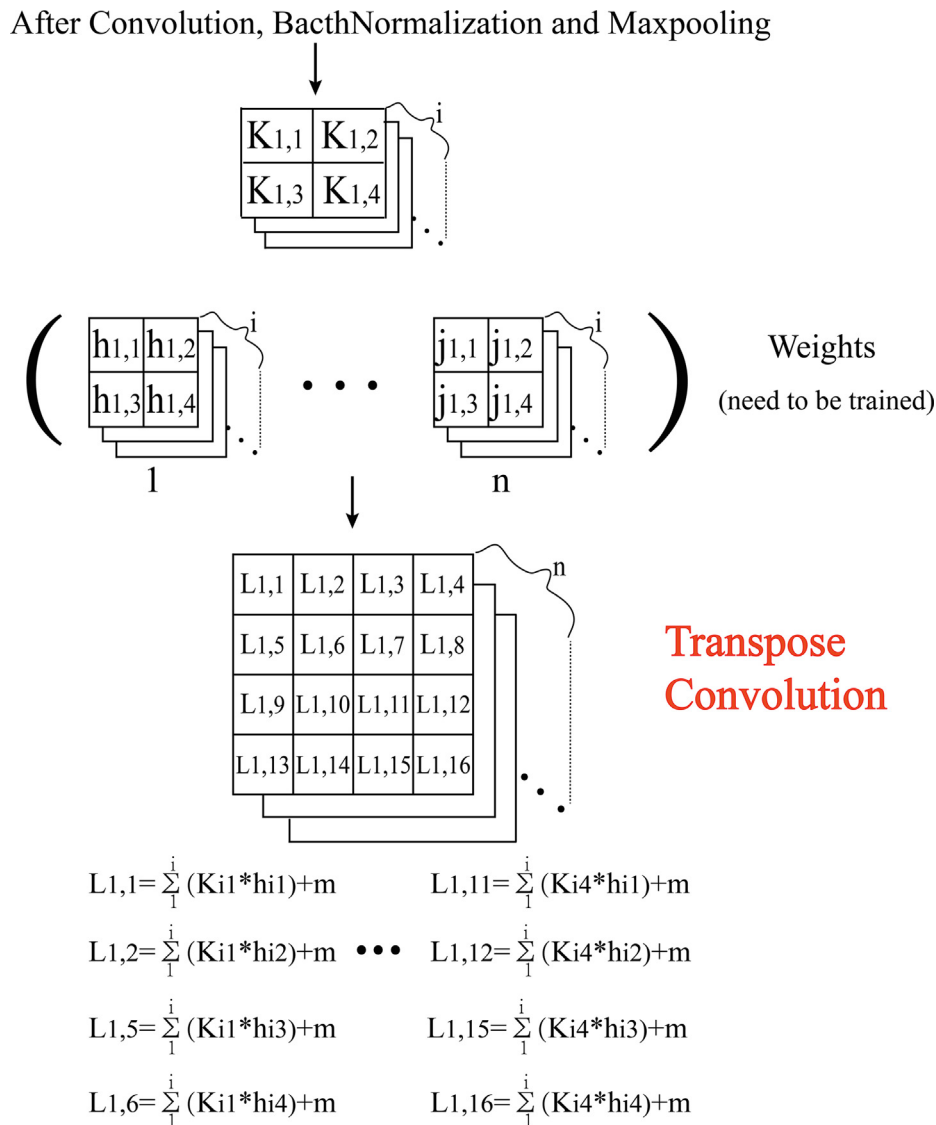
After Convolution, BacthNormalization and Maxpooling

$$L1,1 = \sum_{1}^{i} (Ki1*hi1)+m \qquad L1,11 = \sum_{1}^{i} (Ki4*hi1)+m$$

$$L1,2 = \sum_{1}^{i} (Ki1*hi2)+m \quad \bullet\bullet\bullet \quad L1,12 = \sum_{1}^{i} (Ki4*hi2)+m$$

$$L1,5 = \sum_{1}^{i} (Ki1*hi3)+m \qquad L1,15 = \sum_{1}^{i} (Ki4*hi3)+m$$

$$L1,6 = \sum_{1}^{i} (Ki1*hi4)+m \qquad L1,16 = \sum_{1}^{i} (Ki4*hi4)+m$$

Fig. 4. Detailed schematic diagram of the Transpose Convolution layer.

photos drops down to 400. However, the accuracy of the traditional mode dropped down quickly when the number of training photos was less than 1000 from 92% to 67%.

In order to further explore the ability of our TCNN mode, we randomly selected 400 photos from 3,000 photos, 5 times, to make the training data set and used the unique test set mention above (Fig. 6). After five experiments, we found that when the size of the training data set was 400 photos, the accuracies of the training data sets can all reach 100% after more than 300 epochs' training. The accuracies of the test data sets are no smaller than 97% after more than 400 epochs' training. Meanwhile, through monitoring the loss function of each experiment, we found that the overfitting of the network was slight. The loss function of the training data sets all drops approach 0 after 200 epochs. The loss function of the test data set is no higher than 0.2 after 400 epochs. Therefore, we believe that our TCNN mode can accomplish the classification task very well and efficiently, when only 400 photos are taken as the training data set.

When the number of training data set decreased to 300 (i.e. 300 photos were randomly selected from 3,000 photos for three times), we found that the TCNN mode can still maintain a satisfactory accuracy for all three samplings (Fig. 7). The training sets accuracies and test sets accuracies are no less than 100% and 93% respec-

tively. The training set losses can drop approach 0. However, the test set losses are variable. The best one is 0.1018, but the worst is 0.9217 and after 500 epochs. It can be considered that the TCNN mode has already appeared overfitting, when the training set only has 300 photos. Overfitting happens when the training dataset is too small, so that the TCNN system cannot operate at satisfactory accuracy on the test set. When the number of training set dropped to 200, due to the large number of trainable parameters, the performance of the TCNN on the test set was poor, although it still fit well in the training set. The test set accuracy was less than 50 percent. Not only the loss function of test set is much higher than that of training set, but the accuracy of test set is much lower than that of training set. When the number of training set dropped to 100, TCNN can hardly learn any characteristics on the training set.

It has been shown above that when the number of training sets is 400, the test set accuracy can be maintained while overfitting can be reduced in three kinds of brachiopods identification. To further exploring whether our model has the potential to be extended to four types of brachiopods fossil identification, we add another type of brachiopod, *Obolidae Gen. et* sp. *indet*, in our testing. Unfortunately, we only have 146 photos for this species of brachiopod. So, 146 photos were randomly selected from each of previous three type brachiopods and constitute the 584 photos data set. 100 pho-
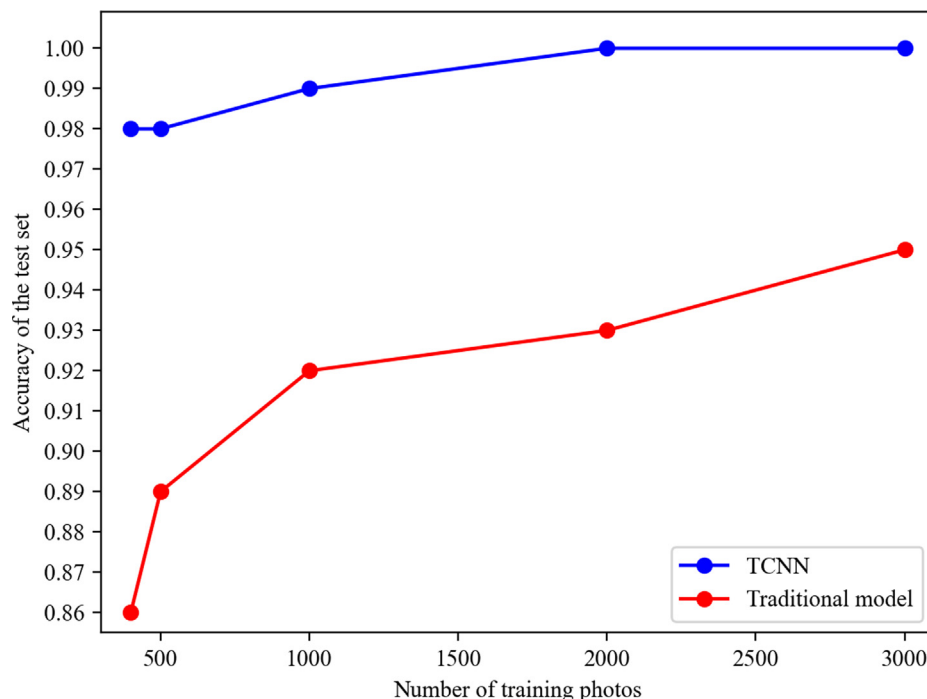
Fig. 5. The comparison of accuracy between traditional convolutional neural network and TCNN model under different sizes of training sets. When the size of the training set gradually decreases from 3000 photos to 400 photos, it can be seen that the accuracy of the traditional convolutional neural network drops significantly, while TCNN can still maintain the accuracy of 98%.

tos were randomly picked out of the data set to be the test set. The rest of the 484 photos automatically become the training set. We didn't change any structure of the TCNN mode and only adjusted the number of neurons in the output layer from three to four. After training, the test set got the accuracy of 98% and the overfitting phenomenon was very slight.

To further explore whether our model has the potential to be extended to more types of brachiopod fossil identification, we then added one more type of brachiopod, *Palaeostrophia jingxiensis* in our testing procedure. Because of the limitation of the number of photos of *Obolidae Gen. et* sp. *indet*, all 146 photos of *Obolidae Gen. et* sp. *indet* were used. 146 photos were randomly selected from each of previous three type brachiopods and *Palaeostrophia jingxiensis*. All those photos constitute a data set of 730 photos. 100 photos were randomly picked out of the data set to be the test set. The rest 630 photos form the training set. We did not change any structure of the TCNN mode and only adjusted the number of neurons in the output layer from four to five. After training, we found that the accuracy of the test set is 97%.

5. Discussion

Due to the large number of trainable parameters, our small training data sets are obviously not big enough to enable the traditional linear convolutional neural network to learn enough features of the data set, so the accuracy of the testing set is poor. In order to make the neural network learn more features from our small training data set, we want to bring in the "upsampling" layer inspired by U-NET model. Meanwhile, the U-NET mode applied many "upsampling" layers which increase the size of the neural network. It might also cause overfitting while the training data set is small. So, we chose to add only one transpose convolution layer, the "upsampling" layer, to the traditional network. Then, we superimpose the outputs of the transpose convolution layer with the 6th Convolution layer after BatchNormalization. The transpose convolution layer is 'upsampling' the output of the 8th

BatchNormalization Layer, so that its length, width and number of channels are the same as the output of the 6th BatchNormalization Layer, then we concated them in the channel direction. The advantage of mixing those two layers is that the different levels of features are sufficiently mixed to enable the neural network to fully learn and utilize these features.

Compared with the traditional model, the accuracy of the neural network we used is much higher, indicating that for the classification of brachiopod fossils, the results obtained by fully mixing the global features and local features are improved. Also the speed of convergence of the network we used is much greater than that of the traditional linear convolutional neural network. When the training data size is 3000, the network we used has been able to achieve and stabilize the accuracy at 100% in less than 50 epochs. When the training data size is 400 photos, although our model took more epochs to achieve convergence, the accuracy of the test set is much higher than that of the traditional model. Because of the difficulty in collecting fossil samples, it is important to maintain a high accuracy when the sample size is small.

Unlike other convolutional neural networks that usually use larger batch size, as large as memory and GPU memory allow, our neural network obtains a higher accuracy when using smaller batch size (Keskar et al., 2016). It means that running our mode required lower computer performance and easier to apply to the computer with relatively smaller memory and GPU memory in brachiopod fossil identification.

Based on all the tests mentioned above, we found that our TCNN mode has good applicability to keep 97% identify accuracy while overfitting can be reduced in the 630 photos per 5 brachiopod species. Due to our brachiopod sample limitations, there are not enough data to put more brachiopods species into the identifying test. This work will require more brachiopod species data to further test our model.

Based on our test, we preliminarily assume that if one brachiopod species has less than around 100 specimens, then it is not possible to achieve satisfactory identification accuracy in our
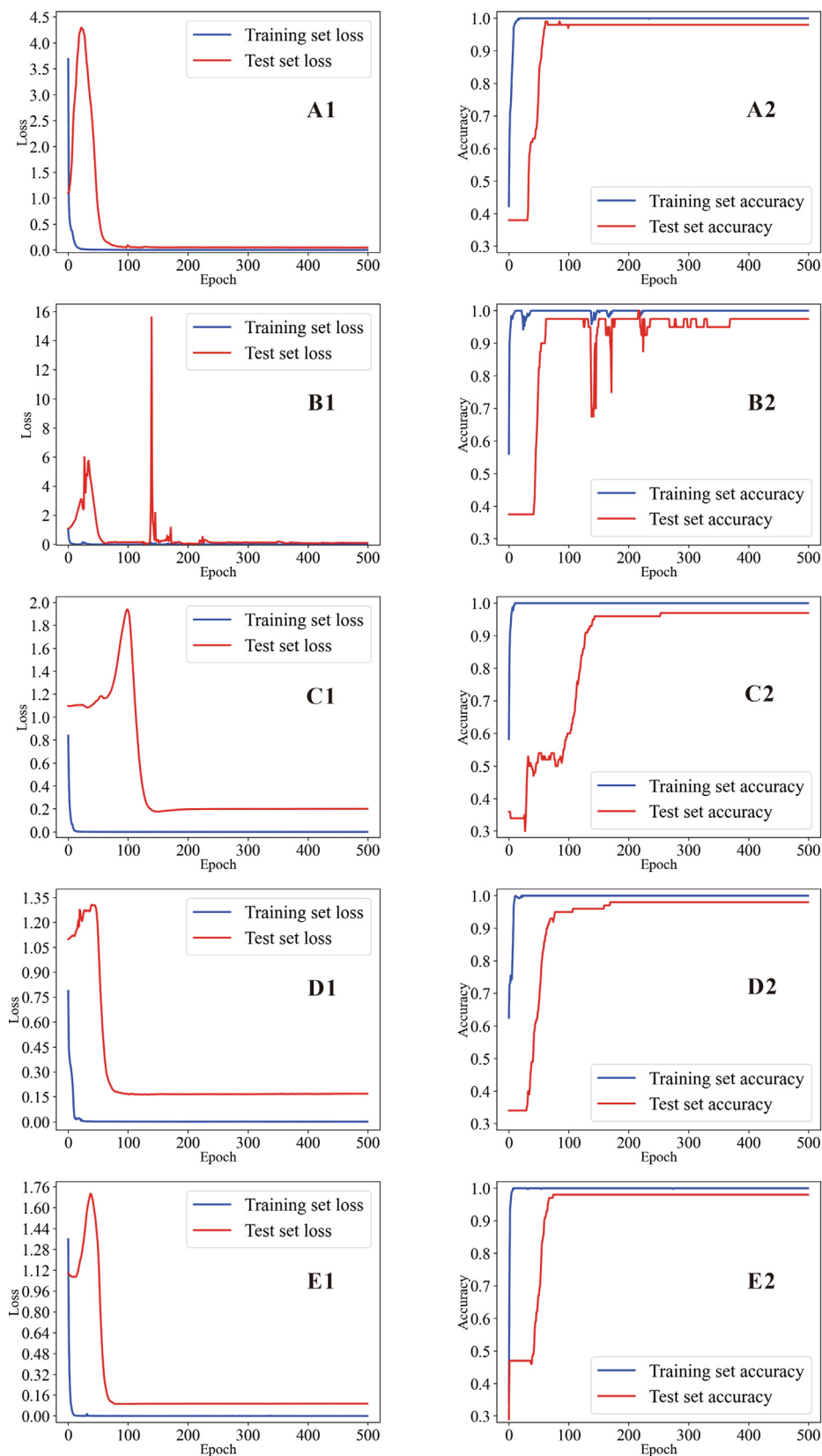
Fig. 6. Plots showing that when the size of training sets is 400, five training sets are randomly selected Figures A1 to E1 correspond to the correct rates of training set and test set, and Figures A2 to E2 correspond to the loss functions of training set and test set. At this point, there is no obvious overfitting.

TCNN model. This limitation prevents the application of TCNN to identification of species that have a small number of specimens, which is why we take only 5 species into account for this study.

Some parameters need to be set manually in the TCNN model: the learning rate, the number of neurons in each hidden layer, and the activation function. The selection of these parameters is
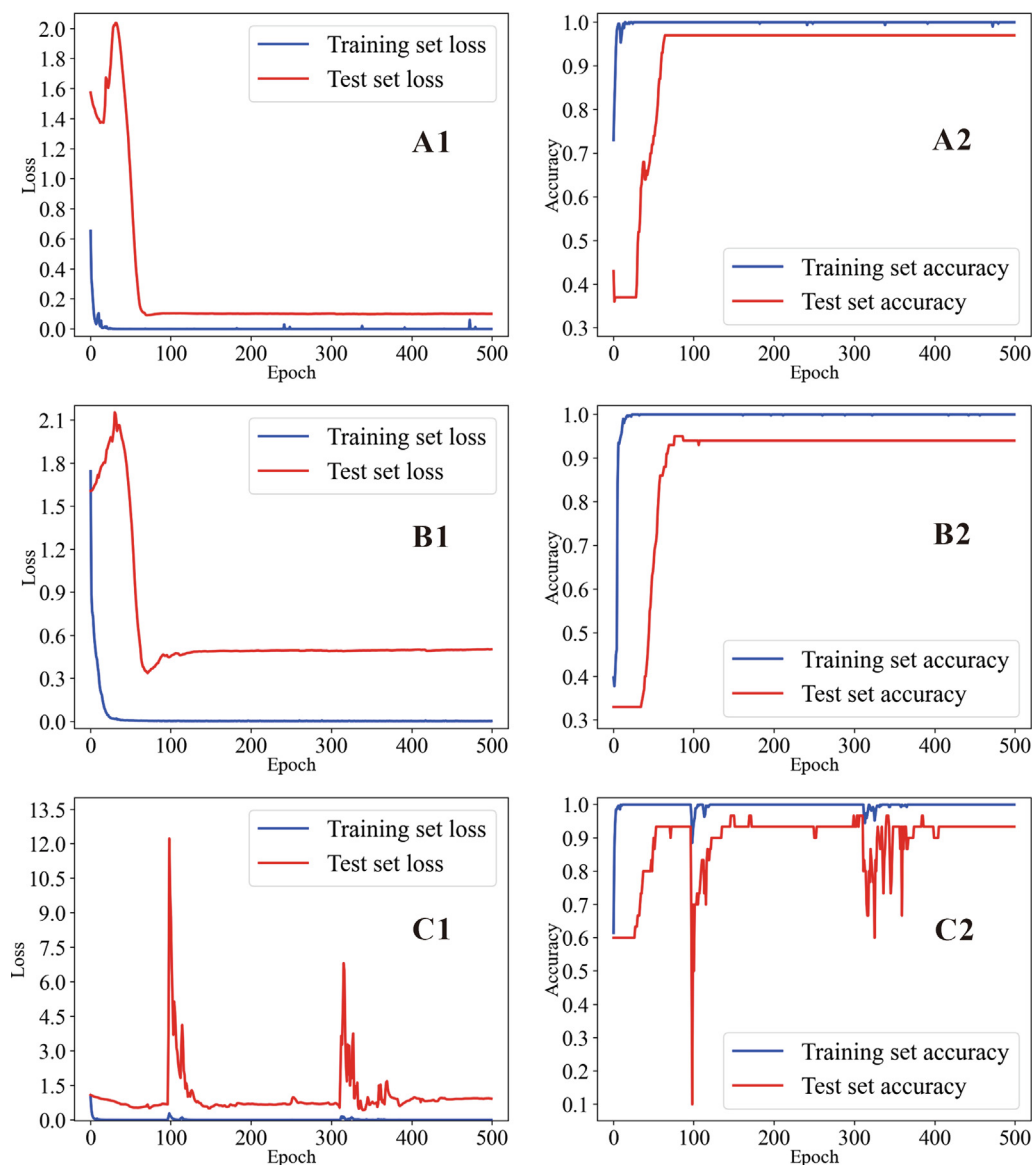
Fig. 7. Plots showing that when the size of training sets is 300, three training sets are randomly selected. Figures A1 to C1 correspond to the correct rates of training set and test set, and Figures A2 to C2 correspond to the loss functions of training set and test set. At this point, obvious overfitting occurs.

more dependent on personal experience, so far there is still a lack of scientific and effective guiding theory. Therefore, a lot of time is needed to adjust these parameters to achieve satisfactory accuracy of the TCNN model.

Another limitation is that we could not quantify how complete do the specimens have to be for accurate identification. It remains uncertain as to whether broken specimens can be identified or not. Our data contain some broken specimens, although most of them are complete shells; nevertheless, many are not perfectly complete. The test data are randomly picked from our collection, so theoretically a few broken specimens may be included in the test data, so the overall test accuracy includes those broken specimens. We assume if an incomplete specimen has enough unique features then it could be accurately identified, which may be possible in future work.

6. Conclusions

Overall, the TCNN model was proven to be very successful in brachiopod identification at genus and species level based on our

data. Compared with the traditional CNN, the "upsampling" Transpose Convolutional Layer mixed with a Convolutional Layer is the core feature of the TCNN, which makes a notable increase in accuracy of identification of the brachiopods based on a relatively small number of brachiopod images. Our tests also indicated that the TCNN has great potential to be applied to automatically identify brachiopod fossils and might become a reliable taxonomic tool that could be applied to a wide range of fossil organisms.

Credit Author Statement

Haizhou Wang and **Chufan Li** designed the research and performed the modelling and simulation; **Haizhou Wang, Zhifei Zhang, Lars E. Holmer and Yang Zhang** conducted fieldwork and sample identification. All authors contributed to the discussion and manuscript writing.

Declaration of Competing Interest

The authors declare that they have no known competing financial interests or personal relationships that could have appeared to influence the work reported in this paper.

Acknowledgements

References

Abadi, M., 2016. TensorFlow: Learning Functions at Scale. Acm Sigplan Notices 51 (9).

Redmon, J., Divvala, S., Girshick, R., Farhadi, A., 2016. You only look once: Unified, real-time object detection. IEEE Conference on Computer Vision and Pattern Recognition (CVPR) 2016, 779–788.

Cui, H., Zhang, H., Ganger, G.R., Gibbons, P.B., Xing, E.P., 2016. GeePS: Scalable deep learning on distributed GPUs with a GPU-specialized parameter server. Eleventh European Conference on Computer Systems, 1–40.

Giusti, A., Cirean, D.C., Masci, J., Gambardella, L.M., Schmidhuber, J., 2014. Fast Image Scanning with Deep Max-Pooling Convolutional Neural Networks. IEEE International Conference on Image Processing 2013, 1–12.

Glorot, X., Bengio, Y., 2010. Understanding the difficulty of training deep feedforward neural networks. In: Proceedings of the thirteenth international conference on artificial intelligence and statistics, pp. 249–256.

Goodfellow, I.J., Pouget-Abadie, J., Mirza, M., Xu, B., Warde-Farley, D., Ozair, S., Courville, A., Bengio, Y., 2014. Generative Adversarial Networks. In: Proceedings of 27th International Conference on Neural Information Processing Systems, pp. 2672–2680.

He, K.M., Zhang, X.Y., Ren, S.Q., Sun, J., 2016. Deep Residual Learning for Image Recognition. IEEE Conference on Computer Vision and Pattern Recognition (CVPR) 2016, 770–778.

Hinton, G.E., Salakhutdinov, R.R., 2006. Reducing the Dimensionality of Data with Neural Networks. Science 313, 504–507.

Hochreiter, S., Schmidhuber, J., 1997. Long Short-Term Memory. Neural Comput. 9 (8), 1735–1780.

Ioffe, S., Szegedy, C., 2015. Batch Normalization: Accelerating Deep Network Training by Reducing Internal Covariate Shift. Proceedings of the 32nd International Conference on Machine Learning 37, 448-456.

Jia, Y., Shelhamer, E., Donahue, J., Karayev, S., Long, J., Girshick, R., Guadarrama, S., Darrell, T., 2014. Caffe: Convolutional Architecture for Fast Feature Embedding. Proceedings of the 22nd ACM international conference on Multimedia, Orlando, Florida, USA. 675-678.

Keskar, N.S., Nocedal, J., Tang, P.T.P., Mudigere, D., Smelyanskiy, M., 2016. On large-batch training for deep learning: Generalization gap and sharp minima. arXiv preprint at https://arxiv.org/abs/1609.04836.

Kingma, D., Ba, J., 2014. Adam: A Method for Stochastic Optimization. arXiv preprint at https://arxiv.org/abs/1412.6980.

Krizhevsky, A., Sutskever, I., Hinton, G.E., 2017. ImageNet Classification with Deep Convolutional Neural Networks. Commun. ACM 60 (6), 84–90.

Le, Q.V., Ngiam, J., Coates, A., Lahiri, A., Ng, A.Y., 2011. On Optimization Methods for Deep Learning. In: Proceedings of the 28th International Conference on Machine Learning, pp. 265–272.

Lecun, Y., Bottou, L., Bengio, Y., Haffner, P., 1998. Gradient-based learning applied to document recognition. Proc. IEEE 86 (11), 2278–2324.

Li, X., Chen, S., Hu, X.L., Yang, J., 2019. Understanding the Disharmony between Dropout and Batch Normalization by Variance Shift. 2019 IEEE/CVF Conference on Computer Vision and Pattern Recognition (CVPR 2019), 2677-2685.

Long, J., Shelhamer, E., Darrell, T., 2015. Fully Convolutional Networks for Semantic Segmentation. IEEE Conference on Computer Vision and Pattern Recognition (CVPR) 2015, 3431–3440.

Ronneberger, O., Fischer, P., Brox, T., 2015. U-Net: Convolutional Networks for Biomedical Image Segmentation. Medical Image Computing and Computer-Assisted Intervention, Pt Iii 9351, 234–241.

Salakhutdinov, R., Mnih, A., Hinton, G., 2007. Restricted Boltzmann machines for collaborative filtering. Proceedings of the 24th International Conference on Machine Learning.

Shen, W., Zhou, M., Yang, F., Yang, C., Tian, J., 2015. Multi-scale Convolutional Neural Networks for Lung Nodule Classification. Proceedings of the 24th International Conference on Information Processing in Medical Imaging, Isle of Skye Scotland.

Silver, D., Huang, A., Maddison, C.J., Guez, A., Sifre, L., van den Driessche, G., Schrittwieser, J., Antonoglou, I., Panneershelvam, V., Lanctot, M., Dieleman, S., Grewe, D., Nham, J., Kalchbrenner, N., Sutskever, I., Lillicrap, T., Leach, M., Kavukcuoglu, K., Graepel, T., Hassabis, D., 2016. Mastering the game of Go with deep neural networks and tree search. Nature 529 (7587), 484–489.

Simonyan, K., Zisserman, A., 2014. Very Deep Convolutional Networks for Large-Scale Image Recognition. arXiv preprint at https://arxiv.org/abs/1409.1556.

Wang, H., Zhang, Z., Holmer, L.E., 2014. Oldest glosselline linguliform brachiopod with soft parts from the Lower Cambrian of Yunnan. Southern China. GFF 136 (4), 539–547.

Zhan, R.B., Jin, J.S., Rong, J.Y., Zhu, X.J., Han, N.R., 2010. Late Cambrian brachiopods from Jingxi, Guangxi Province. South China. Alcheringa 34 (2), 99–133.

Zhang, Z.F., Han, J, Zhang, X.L., Liu, J.N., Shu, D.G., 2003. Pediculate brachiopod Diandongia pista from the Lower Cambrian of South China. Acta Geol. Sin-Engl. 77, 288–293.

Zhang, Z., Han, J., Zhang, X., Liu, J., Shu, D., 2004. Soft-tissue preservation in the Lower Cambrian linguloid brachiopod from South China. Acta Palaeontol. Pol. 49, 259–266.

Zhang, Z.F., 2014. New data on Cambrian (series 2) brachiopods from eastern Yunnan. Northwestern University Press, Northwestern University, pp. 62–64 (in Chinese).